ChemPubSoc Europe

DOI: 10.1002/chem.201903240

CHEMISTRY
A European Journal
Communication

Photochemistry

Introducing LNAzo: More Rigidity for Improved Photocontrol of Oligonucleotide Hybridization**

Nikolai Grebenovsky, Larita Luma, Patricia Müller, and Alexander Heckel*[a]

Abstract: Oligonucleotide-based therapeutics have made rapid progress in clinical treatment of a variety of disease indications. Since most therapeutic oligonucleotides serve more than just one function and tend to have a prolonged lifetime, spatio-temporal control of these functions would be desirable. Photoswitches like azobenzene have proven themselves as useful tools in this matter. Upon irradiation, the photoisomerization of the azobenzene moiety causes destabilization in adjacent base pairs, leading to a decreased hybridization affinity. Since the way the azobenzene is incorporated in the oligonucleotide is of utmost importance, we synthesized locked azobenzene *C*-nucleosides and compared their photocontrol capabilities to established azobenzene *C*-nucleosides in oligonucleotide test-sequences by means of fluorescence-, UV/Vis-, and CD-spectroscopy.

Artificial control of biological function remains one of the most important topics of oligonucleotide chemistry. In living organisms, oligonucleotide hybridization regulates the expression of genes and biosynthesis by revealing the encoded information only when desired. The simple base-pairing rules led to many promising applications in cell biology, pharmacology, or nanotechnology.[1–6] For instance, oligonucleotide therapeutics against miRNA-34a play a major role in controlling cell proliferation.[7] However, miRNA-34a is an important tumor suppressor and corresponding antimiRs have been shown to cause serious adverse effects in off-target tissues in clinical trials[8] and have an in vivo half-life time of up to several weeks.[9]

The need for a convenient method to add spatio-temporal control to therapeutic oligonucleotides led to many studies regarding the distribution, cell uptake, and pharmacokinetics.[10–12] A possible way of gaining control over these effects is the incorporation of light-responsive elements. In contrast to most chemical stimuli, light does not pollute the system, is harmless for biological applications and can be applied with high spatio-temporal control and dose-precision.[13–15] Several examples of photoactivatable antimiRs have been synthesized utilizing photocleavable protecting groups.[16,17] Unfortunately, activation of antimiRs with photocleavable protecting groups is an irreversible process; therefore, adverse effects need to be taken into consideration. To harness the energy of light and translate it into a reversible reaction, a reversible system, which can be switched between different states, is desirable. Photoswitches like spiropyrans,[18,19] hemithioindigos,[20] rhodopsins[21] or azobenzenes[22,23] can isomerize into different isoforms when irradiated with light of corresponding wavelength.

Azobenzenes have a great potential for oligonucleotide applications. They are easy to synthesize,[24] can be custom tailored to the applications requirements,[25] and have already been used in numerous studies involving oligonucleotides.[22,26] Azobenzenes have two distinct photoisomers. The *trans* state azobenzene is planar with no dipole moment[27] and an end-to-end distance and polarity distribution similar to a nucleobase-pair,[26] causing the least possible perturbation while intercalating between neighboring base pairs. Upon irradiation with near-UV light, azobenzenes undergo photoisomerization to form *cis*-azobenzene. Its helical conformation with a dipole moment of approximately 3 Debye can cause steric repulsion in its proximity, which perturbs hydrogen bonds of adjacent

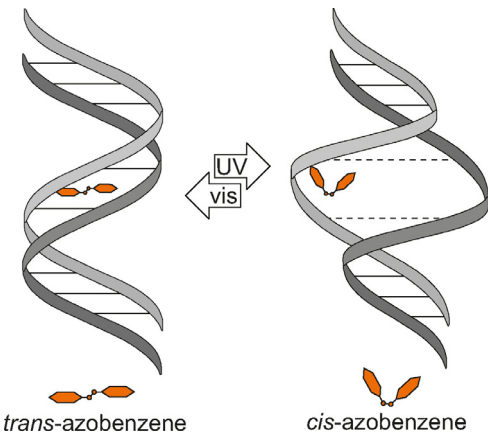

Figure 1. Influence of the azobenzene photoisomerization on an oligonucleotide duplex. In contrast to the planar *trans* state (left) the helical *cis* state (right) leads to a local destabilization, reducing duplex stability.

[a] N. Grebenovsky, L. Luma, P. Müller, Prof. Dr. A. Heckel
Institute for Organic Chemistry and Chemical Biology
Goethe-University Frankfurt
Max-von-Laue-Straße 7, 60438 Frankfurt am Main
(Germany)
E-mail: heckel@uni-frankfurt.de

[**] LNAzo = locked azobenzene C-nucleoside.

Supporting information and the ORCID identification number(s) for the author(s) of this article can be found under: https://doi.org/10.1002/chem.201903240.

base pairs and thereby lowers the hybridization affinity of the oligonucleotide duplex (Figure 1).

One of the biggest tasks in creating photoresponsive oligonucleotides with azobenzenes is the question of how to incorporate the chromophore into the strand. Multiple approaches have been realized to date[26] with the most prominent one being developed by Asanuma et al. in 2001.[28] It consists of a diol-linker derived from *D*-threoninol with azobenzene attached to the side chain by means of an amide bond. This residue can be incorporated into oligonucleotides by standard solid-phase synthesis. This "tAzo" residue has been widely used in many oligonucleotide applications, including photocontrol of enzymatic reactions,[29–31] transcription,[32,33] and DNA nanostructures.[34–36] Despite its ability to stabilize duplexes in the *trans* state and its versatile photocontrol of duplex formation, certain drawbacks like the need for elevated temperatures for optimal switching can limit the scope of application in certain cases.[26]

More recently, a new linker system involving azobenzene *C*-nucleosides has been developed to improve the photocontrol capabilities. This linker system mimics a natural nucleoside, with the nucleobase replaced by the azobenzene chromophore at the anomeric position of the ribose moiety. Azobenzene *C*-nucleosides have been used to control hybridization properties in DNA,[37] RNA,[38] and even DNA-nanostructures.[39]

Despite the fact that DNA-based azobenzene *C*-nucleosides (such as DNAzo, Figure 2a) make better use of the leverage of the azobenzene photoisomerization compared to known linker systems due to the increased rigidity, certain drawbacks have been reported: for example, the combination of deoxyribose and azobenzene penetrates deeper into the stacking region of the duplex compared to acyclic residues.[40] This causes a steric hindrance even in its favored *trans* state, which can be partly addressed by installing abasic sites in the counter strand.[39] Additionally, melting temperature studies suggest that the effect caused by the photoisomerization is lower than expected for such a rigid linker system. A reason for this could be the conformational freedom in the sugar moiety. It is known that ribose can exist in either the 2′- or 3′-*endo* conformation. The intended tension caused by the photoisomerization of azobenzene is possibly lost due to these degrees of conformational freedom rather than being used to force hydrogen bonds out of optimal distance (Figure 2a).

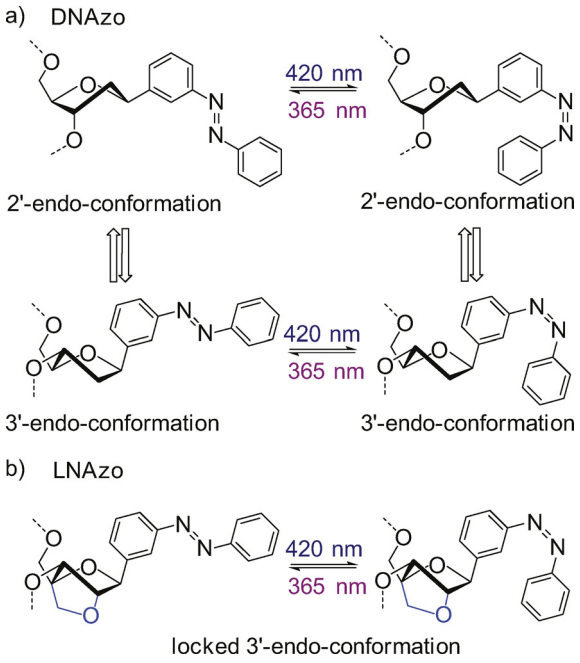

Figure 2. Display of the photoisomerization and conformational changes in a) DNAzo and b) LNAzo.

To overcome these issues we created an azobenzene *C*-nucleoside with a methylene-bridge between the 4′-*C* and 2′-*O* of the ribose unit in analogy to locked nucleic acid building blocks (LNA). This novel locked azobenzene *C*-nucleoside (LNAzo) is conformationally locked in a 3′-*endo* conformation, so that energy loss due to conformational rearrangements is prevented (Figure 2b). With this step we also address the issue of the increased steric repulsion caused by azobenzene *C*-nucleosides, since incorporation of LNA units into oligonucleotides are reported to increase the hybridization affinity by enhanced base stacking and backbone preorganization.[41]

Azobenzenes have been previously incorporated into LNA by attachment through an alkynyl-linker at the C5-position of a locked uridine nucleoside.[42] In this study, positioning and length of the linker causes the azobenzene to be oriented into the major groove, which leads to little change of the hybridization behavior upon irradiation with ΔT_M values of 1 °C. In this matter, locked azobenzene *C*-nucleosides are expected to yield more promising results. The *trans*-azobenzene moiety has to be positioned in the stacking region and a migration of the intentionally bulky *cis*-photoisomer into the minor or major groove has to be prevented.[40]

LNA-type *C*-nucleosides have been synthesized by the groups of Obika[43] and Wengel[44] before. We chose the latter approach as a guideline for the synthesis of LNAzo-phosphoramidites. Starting from aldehyde **1**, which can be synthesized over 11 steps from simple precursors as described in the literature[44,45] (Figure 3), the azobenzene moiety can be introduced by nucleophilic attack as lithiated species, leading to separable (*S*)- and (*R*)-diastereomers **2** and **3**, respectively. After Mitsunobu-type cyclization to form anomers **4** and **5**, deprotection of the alcohol groups led to the free nucleosides **6** and **7**. To incorporate LNAzo building blocks into oligonucleotides by solid-phase synthesis, phosphoramidites were prepared by tritylation (compounds **8** and **9**) and successive phosphitylation (compounds **10** and **11**). The DNAzo phosphoramidite used as reference in this study was synthesized as previously published.[39]

To test the impact of the improved linker system, a model sequence with a 60% GC-content was chosen. A sequence length of 10 nucleotides was chosen in order to evaluate the impact of a single photoswitch incorporated into the oligonucleotide. Fluorescein and Dabcyl residues as fluorophore-quencher pairs were installed at one end of the duplex to obtain melting temperature data from fluorescence readout as well as UV/Vis measurements. For thorough evaluation, the

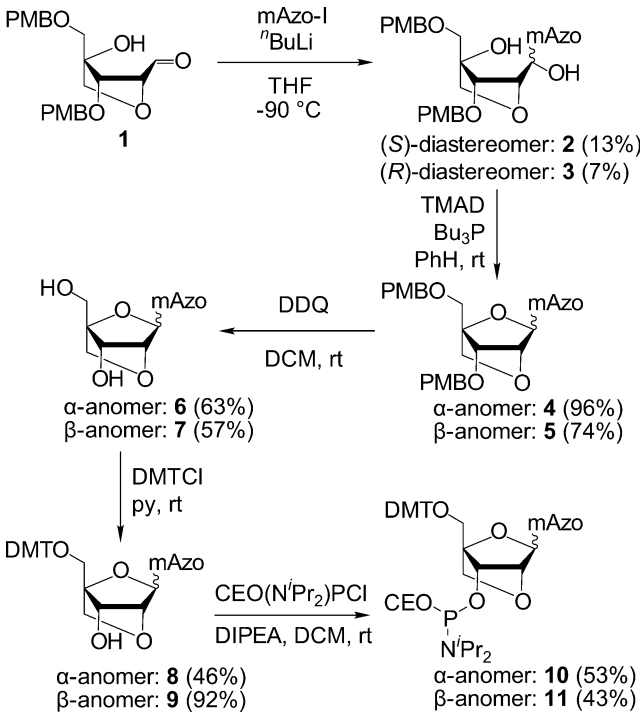

Figure 3. Synthesis of LNAzo-phosphoramidites for oligonucleotide synthesis. Abbreviations: mAzo (*meta*-azobenzyl), PMB (*para*-methoxybenzyl), TMAD (tetramethylazodicarboxamide), DDQ (2,3-dichloro-5,6-dicyanobenzoquinone), DMT (4,4′-dimethoxytrityl), CE (cyanoethyl), DIPEA (diisopropylethylamine).

new LNAzo units were tested in four different oligonucleotide contexts (Figure 4).

At first, the modifications were incorporated into DNA strands with an unmodified DNA strand as binding partner (system 1). The decrease of melting temperature values due to incorporation were between 20.1 °C for LNAzo α and 13.9 °C for LNAzo β, indicating that α-orientation leads to an additional perturbation in a B-helix, whereas the LNAzo β improves stabilization in the duplex by 2.7 °C compared to the established DNAzo residue. The ΔT_M between the respective *cis* and *trans* states vary only a little between DNAzo and LNAzo β. However, LNAzo α did not show any photocontrol within standard deviation. Exchanging the nucleobase corresponding to the *C*-nucleoside on the opposite strand with an abasic site (system 2) afforded an overall increase in melting temperatures by an average of 2 °C. The relative behavior of DNAzo, LNAzo α and LNAzo β remained the same as before. Interestingly, the melting temperature of the wild type control with an abasic site dropped dramatically. Clearly, this construct is thermodynamically more like a 4-mer and a 5-mer duplex connected through a guanosine-linker. This assumption could also be supported by CD-spectroscopy (Supporting Information, section 5). The B-helical character of the duplexes for system 1 were unaltered by incorporation of an azobenzene modification. In system 2, the change in the CD spectrum between wild type and the modified strands was stronger, supporting the previous interpretation of two separate duplexes connected by a linking guanosine. Further investigations on the influence of the abasic site in this sequence context can be found in the Supporting Information, section 7. As it is known that LNA building blocks promote the A-helical character of oligonucleotides, an improved photocontrol could be expected by going from DNA to RNA. In system 3, we investigated the behavior of an azobenzene-modified DNA-strand with an RNA counter strand. The ΔT_M value for DNAzo did not change significantly compared to system 1, but LNAzo β improved by almost 50 % compared to DNAzo. Even LNAzo α showed significant photocontrol under these conditions with ΔT_M values of 2 °C. Finally, by incorporating the azobenzene *C*-nucleoside into an RNA context to form RNA-RNA-duplexes (system 4) the real potential of LNAzo could be seen. Though the ΔT_M values between the *trans* and the *cis* state for DNAzo remained at values around 4 °C, LNAzo β reaches record values of up to 8.6 °C with only one modification in a duplex. Interestingly, photocontrol through LNAzo α decreased again compared to system 3 with ΔT_M values of 1.1 °C. A summary of the values can be seen in Figure 4b and c. More details can be found in the Supporting

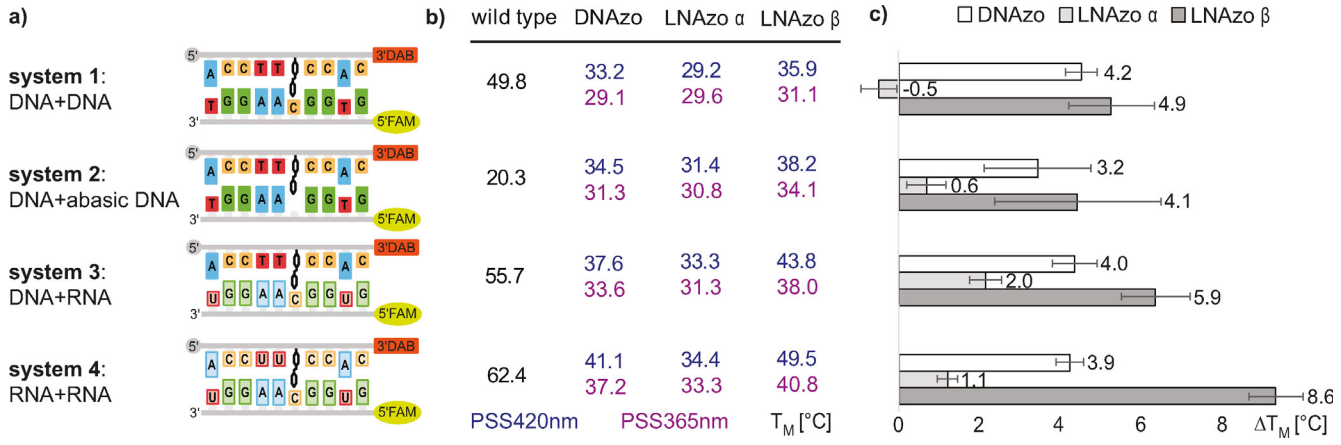

Figure 4. a) Schematic display of the oligonucleotide test systems used in this study. In the case of the wild-type duplexes, the azobenzene moiety was replaced by guanosine; b) summary of the melting temperatures measured by UV/Vis-spectroscopy, samples were irradiated at elevated temperatures, until photostationary state was reached (365 nm indicated in purple/420 nm indicated in blue, values given in °C); c) bar graph of measured ΔT_M values including error bars.

Information, section 4. CD spectroscopy showed the expected transition from a B- to an A-helical character (Supporting Information, section 5). Because LNA building blocks were designed to work best in an A-helical environment it is only reasonable that LNAzo β also works best in the pure RNA context of system 4. In addition to measuring melting curves with UV/Vis-absorption, temperature-dependent fluorescence was measured in a real-time PCR device for all systems in a concentration range of 0.1 to 5 μM. The results were in overall accordance with values from UV/Vis-absorbance. Fluorescence-based melting temperatures are listed in the Supporting Information, section 6.

In summary, we were able to synthesize novel locked azobenzene *C*-nucleosides and evaluate their key characteristics in oligonucleotide test systems. The relatively long (16-steps) synthesis mainly consists of established reactions and especially the steps which are similar to the synthesis of unmodified LNA monomers are already extremely well optimized. We found that, in comparison to established azobenzene *C*-nucleosides, the influence of novel LNAzo β appears to be similar to DNAzo with slightly elevated melting temperatures in a DNA duplex. The superiority of LNAzo β could be shown in an RNA sequence context when RNA counter strands were involved with a maximum ΔT_M of 8.6 °C. LNAzo α showed little to no photocontrol in all systems tested with the lowest melting temperatures in general. This indicates again that orientation of the azobenzene chromophore in the duplex is of utmost importance for reversible photocontrol of oligonucleotide hybridization behavior. With LNAzo β we provide a powerful tool for a defined release of RNA with light as external stimulus, which can be utilized for oligonucleotide-based therapeutics in an antisense oligonucleotide approach in future.

Experimental Section

Organic syntheses including spectroscopic data are described in detail in the Supporting Information, section 1. The oligonucleotide synthesis including mass spectroscopic data are included in Supporting Information section 2. For melting temperature measurements 1 mL samples were prepared with 1 μM of strand and counter strand in 1x PBS-buffer for each modification and each system (16 in total). The absorbance changes at 260 nm were measured by a UV/Vis-spectrometer from JASCO. Samples were irradiated as single strands at elevated temperatures (systems 1–3: 70 °C, system 4: 80 °C) with either 365 nm or 420 nm until photostationary state (PSS) was reached to prevent mismatches. Temperature gradient was 1 °C per min. To avoid effects of hysteresis, melting temperatures were calculated by sigmoidal fit from cooling and heating measurements. At least five independent heating and cooling measurements were performed for precise results. Temperature-dependent fluorescence measurements have been recorded in a PikoReal real-time PCR system from Thermo Scientific. Triplicates were irradiated at 80 °C, then spectra were measured from 80 to 5 °C within one hour. Values given are averaged over these three individual samples.

Acknowledgements

This work was supported by the Deutsche Forschungsgesellschaft through SFB902 (Molecular Principles of RNA-based Regulation). Open access funding enabled and organized by Projekt DEAL.

Conflict of interest

The authors declare no conflict of interest.

Keywords: azo compounds · DNA · oligonucleotides · photochemistry · RNA

[1] X. Shen, D. R. Corey, *Nucleic Acids Res.* **2018**, *46*, 1584 – 1600.
[2] U. Sahin, K. Karikó, Ö. Türeci, *Nat. Rev. Drug Discovery* **2014**, *13*, 759 – 780.
[3] Z. Li, T. M. Rana, *Nat. Rev. Drug Discovery* **2014**, *13*, 622 – 638.
[4] E. Stulz, *Chem. Eur. J.* **2012**, *18*, 4456 – 4469.
[5] F. Hong, F. Zhang, Y. Liu, H. Yan, *Chem. Rev.* **2017**, *117*, 12584 – 12640.
[6] P. Wang, T. A. Meyer, V. Pan, P. K. Dutta, Y. Ke, *Chem* **2017**, *2*, 359 – 382.
[7] C. Mollinari, M. Racaniello, A. Berry, M. Pieri, M. C. de Stefano, A. Cardinale, C. Zona, F. Cirulli, E. Garaci, D. Merlo, *Cell Death Dis.* **2015**, *6*, e1622 – e1622.
[8] A. Farooqi, S. Tabassum, A. Ahmad, *Int. J. Mol. Sci.* **2017**, *18*, 2089.
[9] X. J. Li, Z. J. Ren, J. H. Tang, *Cell Death Dis.* **2014**, *5*, e1327 – e1327.
[10] S. T. Crooke, S. Wang, T. A. Vickers, W. Shen, X. Liang, *Nat. Biotechnol.* **2017**, *35*, 230 – 237.
[11] R. L. Juliano, *Nucleic Acids Res.* **2016**, *44*, 6518 – 6548.
[12] R. S. Geary, D. Norris, R. Yu, C. F. Bennett, *Adv. Drug Delivery Rev.* **2015**, *87*, 46 – 51.
[13] C. Brieke, F. Rohrbach, A. Gottschalk, G. Mayer, A. Heckel, *Angew. Chem. Int. Ed.* **2012**, *51*, 8446 – 8476; *Angew. Chem.* **2012**, *124*, 8572 – 8604.
[14] W. Szymański, J. M. Beierle, H. A. V. Kistemaker, W. A. Velema, B. L. Feringa, *Chem. Rev.* **2013**, *113*, 6114 – 6178.
[15] P. Klán, T. Šolomek, C. G. Bochet, A. Blanc, R. Givens, M. Rubina, V. Popik, A. Kostikov, J. Wirz, *Chem. Rev.* **2013**, *113*, 119 – 191.
[16] T. Lucas, F. Schäfer, P. Müller, S. A. Eming, A. Heckel, S. Dimmeler, *Nat. Commun.* **2017**, *8*, 15162.
[17] F. Schäfer, J. Wagner, A. Knau, S. Dimmeler, A. Heckel, *Angew. Chem. Int. Ed.* **2013**, *52*, 13558 – 13561; *Angew. Chem.* **2013**, *125*, 13801 – 13805.
[18] C. Brieke, A. Heckel, *Chem. Eur. J.* **2013**, *19*, 15726 – 15734.
[19] C. Özçoban, T. Halbritter, S. Steinwand, L.-M. Herzig, J. Kohl-Landgraf, N. Askari, F. Groher, B. Fürtig, C. Richter, H. Schwalbe, B. Suess, J. Wachtveitl, A. Heckel, *Org. Lett.* **2015**, *17*, 1517 – 1520.
[20] S. Wiedbrauk, H. Dube, *Tetrahedron Lett.* **2015**, *56*, 4266 – 4274.
[21] D. Martínez-López, M. Blanco-Lomas, P. J. Campos, D. Sampedro, *Tetrahedron Lett.* **2015**, *56*, 1991 – 1993.
[22] A. S. Lubbe, W. Szymanski, B. L. Feringa, *Chem. Soc. Rev.* **2017**, *46*, 1052 – 1079.
[23] A. A. Beharry, G. A. Woolley, *Chem. Soc. Rev.* **2011**, *40*, 4422.
[24] E. Merino, *Chem. Soc. Rev.* **2011**, *40*, 3835.
[25] M. Dong, A. Babalhavaeji, S. Samanta, A. A. Beharry, G. A. Woolley, *Acc. Chem. Res.* **2015**, *48*, 2662 – 2670.
[26] J. Li, X. Wang, X. Liang, *Chem. Asian J.* **2014**, *9*, 3344 – 3358.
[27] L. Briquet, D. P. Vercauteren, E. A. Perpète, D. Jacquemin, *Chem. Phys. Lett.* **2006**, *417*, 190 – 195.
[28] H. Asanuma, T. Takarada, T. Yoshida, D. Tamaru, X. Liang, M. Komiyama, *Angew. Chem. Int. Ed.* **2001**, *40*, 2671 – 2673; *Angew. Chem.* **2001**, *113*, 2743 – 2745.
[29] A. Yamazawa, X. Liang, H. Asanuma, Makoto. Komiyama, *Angew. Chem. Int. Ed.* **2000**, *39*, 2356 – 2357; *Angew. Chem.* **2000**, *112*, 2446 – 2447.
[30] Y. Liu, Dipankar. Sen, *J. Mol. Biol.* **2004**, *341*, 887 – 892.
[31] X. Liang, K. Fujioka, Hiroyuki. Asanuma, *Chem. Eur. J.* **2011**, *17*, 10388 – 10396.

[32] M. Liu, H. Asanuma, Makoto. Komiyama, *J. Am. Chem. Soc.* **2006**, *128*, 1009 – 1015.
[33] X. Liang, R. Wakuda, K. Fujioka, Hiroyuki. Asanuma, *FEBS J.* **2010**, *277*, 1551 – 1561.
[34] F. Tanaka, T. Mochizuki, X. Liang, H. Asanuma, S. Tanaka, K. Suzuki, S. Kitamura, A. Nishikawa, K. Ui-Tei, M. Hagiya, *Nano Lett.* **2010**, *10*, 3560 – 3565.
[35] Y. Kamiya, H. Asanuma, *Acc. Chem. Res.* **2014**, *47*, 1663 – 1672.
[36] Y. Kamiya, Y. Yamada, T. Muro, K. Matsuura, H. Asanuma, *ChemMedChem* **2017**, *12*, 2016 – 2021.
[37] T. Goldau, K. Murayama, C. Brieke, H. Asanuma, A. Heckel, *Chem. Eur. J.* **2015**, *21*, 17870 – 17876.
[38] T. Goldau, K. Murayama, C. Brieke, S. Steinwand, P. Mondal, M. Biswas, I. Burghardt, J. Wachtveitl, H. Asanuma, A. Heckel, *Chem. Eur. J.* **2015**, *21*, 2845 – 2854.
[39] N. Grebenovsky, T. Goldau, M. Bolte, A. Heckel, *Chem. Eur. J.* **2018**, *24*, 3425 – 3428.
[40] P. Mondal, M. Biswas, T. Goldau, A. Heckel, I. Burghardt, *J. Phys. Chem. B* **2015**, *119*, 11275.
[41] R. Owczarzy, Y. You, C. L. Groth, A. V. Tataurov, *Biochemistry* **2011**, *50*, 9352 – 9367.
[42] K. Morihiro, O. Hasegawa, S. Mori, S. Tsunoda, S. Obika, *Org. Biomol. Chem.* **2015**, *13*, 5209 – 5214.
[43] Y. Hari, S. Obika, M. Sakaki, K. Morio, Y. Yamagata, T. Imanishi, *Tetrahedron* **2002**, *58*, 3051 – 3063.
[44] B. Ravindra Babu, A. K. Prasad, S. Trikha, N. Thorup, V. S. Parmar, J. Wengel, *J. Chem. Soc. Perkin Trans. 1* **2002**, 2509 – 2519.
[45] R. Yamaguchi, T. Imanishi, S. Kohgo, H. Horie, H. Ohrui, *Biosci. Biotechnol. Biochem.* **1999**, *63*, 736 – 742.

Manuscript received: July 16, 2019
Revised manuscript received: August 5, 2019
Accepted manuscript online: August 6, 2019
Version of record online: August 28, 2019

